Effect of Lamp Cycling on Conversion and Stress Development in Ultraviolet-Cured Acrylate Coatings

DIANE M. VAESSEN, FREDERYK A. NGANTUNG, MANUEL L. B. PALACIO, LORRAINE F. FRANCIS, ALON V. MCCORMICK

Department of Chemical Engineering and Materials Science, University of Minnesota–Twin Cities, Minneapolis, Minnesota 55455-0132

Received 21 February 2001; accepted 13 August 2001

ABSTRACT: In radiation-cured acrylate coatings, a high conversion of monomer is generally desired to improve hardness, prevent further slow reaction upon aging, and avoid surface toxicity; however, shrinkage and, consequently, stress in coatings tend to increase with conversion. One route to achieve high conversion while maintaining low coating stress is to promote stress relaxation. In this study, acrylate coatings were cured with a UV lamp that was cycled on and off, varying the period from 2 to 60 min while keeping the total dose constant. All samples reached nearly the same conversion, between 46 and 48% conversion of functional groups, as measured by FTIR spectroscopy. The coating stress (measured with cantilever deflection) at the end of the exposure cycles, however, was lowered from 8 MPa (tension) to less than 3 MPa (tension) as the period was decreased from 60 to 2 min. The cycling had no significant effect on either the coating hardness or the modulus, as measured by a Hysitron triboscope. Stress relaxation and/or slower reaction during the dark periods are the likely causes for the lower coating stress. It was advantageous to introduce dark periods early in the processing. © 2002 Wiley Periodicals, Inc. J Appl Polym Sci 84: 2784–2793, 2002

Key words: UV-lamp cycling; optimize radiation curing; stress relaxation; mechanical properties

INTRODUCTION

Photopolymerization of multifunctional acrylates coatings, initiated with ultraviolet (UV) light, is a rapid method for converting liquid monomers and oligomers into crosslinked, glassy polymer networks at room temperature. Acrylate coatings can be formulated without solvent, leading to minimal volatile organic compound emission and reduced energy requirements during processing. The high mechanical strength and good solvent resistance of the resulting crosslinked polymers have led to their application as protective layers, adhesives, dental restorative materials, and photoresists.[1–4] Given the demands of applications like these, there is an ongoing need to achieve high conversion while minimizing coating stress to avoid defects such as peeling, curling, cracking, crazing, rippling, and bending.[5–8]

Shrinkage usually occurs during polymerization because the polymer network formed is usually denser than the unreacted monomer. Because the coating adheres to a rigid substrate,

Correspondence to: A. McCormick (mccormic@cems.umn.edu).

Contract grant sponsor: Industrial Partnership for Research in Interfacial and Materials Engineering (University of Minnesota).

Contract grant sponsor: Intel Corporation.

Journal of Applied Polymer Science, Vol. 84, 2784–2793 (2002)

though, shrinkage (after solidification) can occur only in the thickness direction. Frustration of in-plane shrinkage leads to a tensile stress. However, at the same time that stress accumulates, it can be relaxed by processes such as molecular motion and flow. The measured stress at any time is the result of the competition between stress buildup from frustrated shrinkage and stress relief from relaxation. In UV-cured glassy acrylate crosslinked coatings, the final coating stress can be on the order of 2–30 MPa.[8,9]

In many UV-cured systems, a high crosslink density (i.e., high conversion) is desired to improve hardness and solvent resistance.[10–12] However, shrinkage and the formation of defects generally increase with conversion.[8,11,13–15] Examples of this are found in the fabrication of optical disk and photoresist coatings. For these coatings, a high conversion is important for high modulus, pencil hardness, and abrasion resistance and to avoid outgassing of unreacted monomers and photoinitiators, which can contaminate the atmosphere and/or corrode metal underlayers. However, excessive stress buildup resulting from polymerization shrinkage can cause buckling, cracking, and delamination of the polymer coating.[11,12] Clearly it is an optimization problem to balance increasing conversion against increasing stress.

A number of processing variables have already been shown to influence conversion[8,9,16–21] and stress development[8,9] in UV-cured acrylate coatings subjected to continuous radiation exposure: monomer functionality, photoinitiator concentration, coating thickness, light intensity and wavelength, and curing temperature. However, the effects of imposing a time-varying radiation pattern on conversion, stress development, and mechanical properties have received little attention in the open literature, although such techniques are often used in commercial practice.

In this study we examine the effects of the simplest time-varying exposure sequence: cycling the UV lamp *on* and *off* (square wave) during the processing. During the lamp *on* times, the conversion increases rapidly but with the penalty of increasing stress. During the *off* times, the curing reactions proceed much more slowly and there is opportunity for stress relaxation to occur. We investigate the effect of the duration of the dark period on its ability to effectively reduce stress. We also examine whether comparable conversion, hardness, and modulus can be achieved when incorporating dark reaction periods.

TMPTA

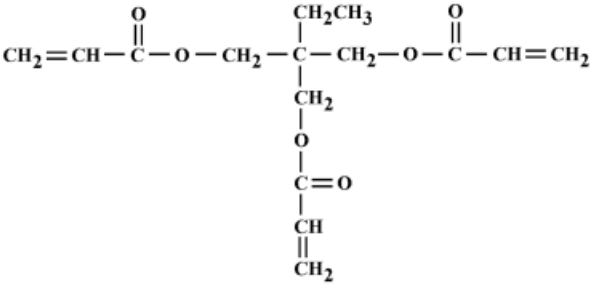

DMPA

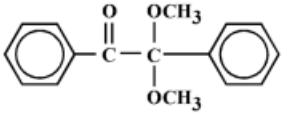

Figure 1 Chemical structures of TMPTA and DMPA.

EXPERIMENTAL

Sample Preparation and Curing Conditions

In the present curing study, trimethylol propane triacrylate (TMPTA; Aldrich Chemical, Milwaukee, WI) was the monomer and 2,2-dimethoxy-2-phenylacetophenone (DMPA; Aldrich), the photoinitiator. The chemical structures are shown in Figure 1. The photoinitiator was added to the monomer liquid in the dark to limit preexperimental curing. The photoinitiator concentration was 0.005 (expressed as the ratio of moles of DMPA to total moles of double bonds). Curing took place at room temperature ($\sim$ 21°C) and in a nitrogen atmosphere to minimize oxygen inhibition of radicals.

A 365-nm UV lamp (Ultracure 100 SS Plus; EFOS, Mississagua, Ontario, Canada) was used to irradiate the samples with a light intensity of 100 μW/cm^2 (unless otherwise noted). The UV intensity of the 365-nm radiation was monitored with a digital radiometer (Spectronics, Westbury, NY). A low light intensity (compared to that of those used in industrial applications) was selected to allow observation of the transient behavior of conversion and stress development (i.e., ultrafast curing was not desired). Under these conditions, the predicted light attenuation through the film thickness (50 μm) was estimated to be less than 3%.

For all but one sample, the UV-exposure cycle consisted of equal intervals of light and dark (i.e., *X* min *on*/*X* min *off*) with an *on*-interval intensity of 100 μW/cm^2. The UV lamp itself was on the

entire time; however, a shutter was used to impose the on/off exposures. If the UV lamp were turned on and off, the lamp's warm-up time would have been an issue. The total time for the experiment was held constant at 1 h. The cumulative on and off times therefore totaled 30 min each. The on/off interval X was varied between 1 and 30 min. For example, with $X = 1$ min, the UV lamp was (*on* 1 min/*off* 1 min) 30 times. Henceforth, $2X$ will be referred to as the *period,* but for convenience, results will be presented and discussed in terms of the *half-cycle time* (X). Note that if the period becomes very small compared to the system's characteristic chemical reaction times, it is as though the system were exposed to an average intensity. This is discussed in more detail in the literature.[22,23] Therefore, the case of 50 μW/cm^2 and 1 h of continuous exposure was also investigated because it represents the limiting case as the period $2X$ approaches zero. In all cases, the total radiation dose was 0.18 J/cm^2.

Stress Measurement

An automated draw-down coater was used to meter coating thickness at a constant coating speed (0.70 cm/s). The final coating thickness in all cases was 50 μm ($\pm$2 μm), as measured with a micrometer (Model 543-253B, 7004; Mitutoyo Corp., Naucalpan, Mexico). Stress development was monitored using a controlled-environment stress-measurement apparatus based on the cantilever deflection measurement principle.[24] Coatings were prepared on steel feeler gauge stock (thickness 0.35 $\pm$ 0.005 mm, clamped dimensions 45 $\times$ 6 mm; L. S. Starrett, Athol, MA). Deflection was measured with an optical lever consisting of a small HeNe laser, a position-sensitive photodiode (DL-10; UDT Sensors, Hawthorne, CA), and various intermediary optics. All data were acquired via computer. The average in-plane stress in the coating was calculated from the cantilever beam bending equation

$$\sigma = \frac{E_S t^3 d}{3cL^2(t + c)(1 - \nu_S)} \quad (1)$$

where E_S and ν_S are the Young's modulus and Poisson's ratio of the substrate, respectively; t and L are the thickness and clamped length of the substrate, respectively; c is the coating thickness; and d is the end deflection of the cantilever. The derivation of eq. (1) with assumptions and experimental constraints is given elsewhere.[25–27]

Conversion Measurement

A Magna 750II FTIR (Nicolet Instruments, Madison, WI) in transmission mode was used to monitor conversion during cure. Samples were sandwiched between two NaCl plates separated by a 0.025 $\times$ 25 mm Teflon spacer (SpectraTech, Shelton, CT) and were then UV-cured inside the instrument (in a nitrogen atmosphere at room temperature). Spectra were acquired and the fractional conversion of double bonds was obtained by monitoring the drop in the C=C absorbance peak area (peaks at 1635 and 1619 cm^{-1}). To directly compare the conversion and stress measurements, the layer of acrylate between the salt plates was made half as thick as the coating used in the stress measurement, to account for reflection of photons from the steel substrates during stress measurement.

The relative final conversion was also determined directly for the coatings from the stress measurement apparatus using diffuse reflectance infrared Fourier transform spectroscopy (DRIFTS). Coated samples were abraded with 320-grit SiC paper (SpectraTech) so that material from the coating surface adhered to the SiC paper, which was then analyzed by DRIFTS. Successive layers (three to five per sample) were transferred onto the SiC paper so that the average extent of cure through the thickness could be calculated and compared to that obtained by transmission FTIR. However, this average could be calculated using data from only the top half of the film because the sanding process triggered film delamination below the 25-μm point. Three to six samples from each coating were obtained and two to three coatings were tested for each cure pathway.

Absorbance values using DRIFTS depend on the quantity of sample; therefore, C=C peak areas were normalized using the 1748 cm^{-1} carbonyl peak. Absolute conversion of the coatings could not be calculated because spectral interference from the SiC paper broadened and shifted the carbonyl peak, as shown in Figure 2. This problem was discussed by Dumont and Depecker[28] and Moradi et al.[29]; these researchers recommend depositing nonabsorbing powder on the sample surface to decrease the penetration depth of the incident beam and to increase the irradiated surface by lateral expansion of the beam in the nonabsorbing material. In this study, however, when nonabsorbing spectral-grade KBr was used, the percentage transmission was severely reduced. Moreover, samples with KBr

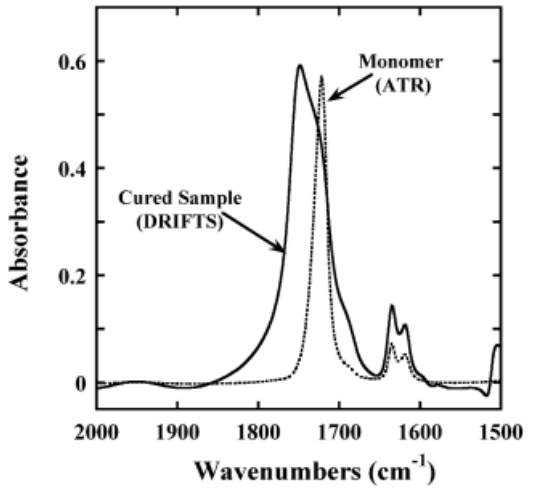

Figure 2 Spectral interference of SiC using DRIFTS leads to broader and shifted carbonyl peak for cured samples. Monomer spectrum was obtained by attenuated total reflectance (ATR).

needed very long purge times to remove interference of water peaks, and there was concern that samples be tested quickly to minimize the error in measurements caused by further reaction. For these two reasons, relative final conversion, not absolute final conversion, is reported. A spectrum of the abrasive paper was used as the background. DRIFTS tests were performed on samples immediately after indentation experiments, which are discussed in the next section. Area ratios were analyzed using a one-way analysis of variance (ANOVA) and the Tukey–Kramer multiple comparison test ($p < 0.05$) to assess differences in the final extent of conversion.

Hardness and Modulus Measurement

A Hysitron triboscope[30] with a diamond tip Berkovich indenter (radius = 1 μm) was used to measure the hardness and reduced modulus of the coatings cured by the different exposure pathways. To minimize the error resulting from changing properties attributed to further cure or physical aging, indentation was performed in darkness within 90 min after cure. Transmission FTIR results showed that conversion increased no more than 2% during this 90-min dark period. The trapezoidal-type load profiles consisted of loading at 4000 μN for 1 s, holding for 30 s, and then unloading in 1 s. Under these conditions, the indenter tip penetrated less than 2% into the film. The hardness of the coatings was calculated using the equation

$$H = P/A_c \tag{2}$$

where A_c is the contact area between the indenter and the film at load P. The reduced modulus E_r for all samples was determined based on a method developed by Doerner and Nix[31] and can be expressed as

$$E_r = \frac{\pi}{2^{1/2}} \frac{dP}{dh} \frac{1}{A_c^{1/2}} \tag{3}$$

where dP/dh is the tangent to the curve P versus h (depth) at the onset of unloading. The reduced modulus can also be expressed as

$$\frac{1}{E_r} = \frac{1 - \nu^2}{E} + \frac{1 - \nu_i^2}{E_i} \tag{4}$$

where E and ν are the Young's modulus and Poisson's ratio for the sample, respectively; and E_i and ν_i are the same parameters for the indenter. When $E_i \gg E$, eq. (4) reduces to

$$E_r = \frac{E}{1 - \nu^2} \tag{5}$$

Ten to 20 indents were made on each coating and the hardness and modulus values were then averaged to obtain a mean hardness and modulus for that coating. The hardness and modulus for the two or three specimens for a cured pathway were then averaged to obtain a group hardness and modulus. These data were analyzed using a one-way ANOVA and the Tukey–Kramer multiple comparison test ($p < 0.05$).

RESULTS AND DISCUSSION

Conversion: Transmission FTIR

Figure 3(a) shows transmission FTIR data for conversion as a function of time during the different curing sequences. For each of the samples, conversion increases rapidly at early times because diffusion coefficients of monomers and radicals are high in the liquid and rubbery states, but conversion increases less rapidly later in the processing because crosslinking and vitrification slow diffusion.[8,9,16–21,32–36] Figure 3(a) suggests that the division between these two regimes is at about 35% conversion. For all curing sequences examined, the final conversion was found to be in

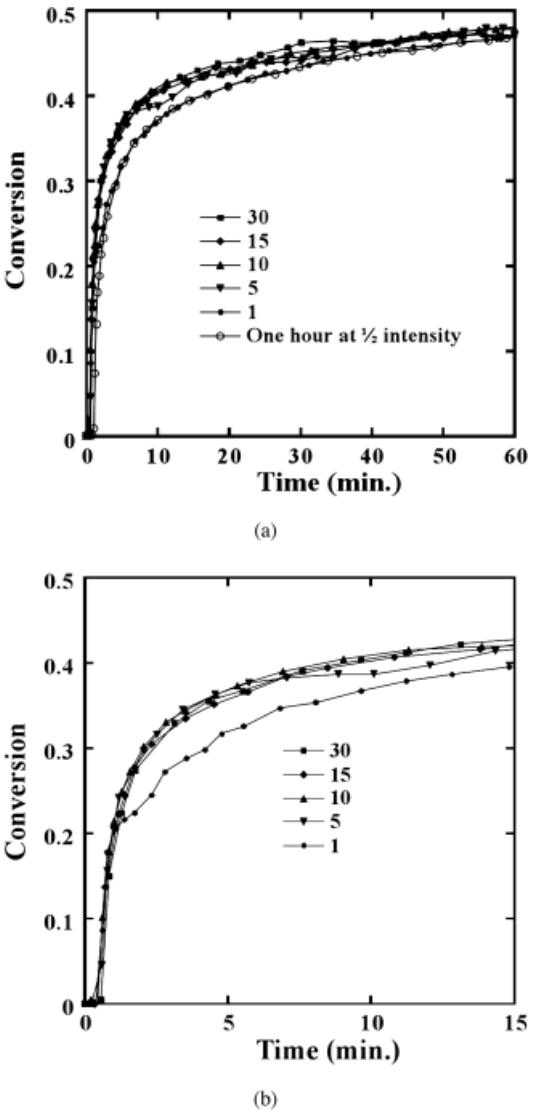

Figure 3 (a) Conversion (transmission FTIR) is not affected by the cycling and depends only on the dose of UV. Plot of conversion in magnitude, labeling with half-cycle times (in minutes), with total dose = 0.18 J/cm^2 for all cases. Each data point represents the conversion obtained from one FTIR scan. A line connecting points represents the interpolated conversion between points. (b) Conversion at early times shows separation between the 5-, 10-, 15-, and 30-min half-cycle time curves and the 1-min half-cycle time curve. The coating exposed to a 1-min half-cycle time is different because the lamp is first turned off before vitrification has occurred. Each data point represents the conversion obtained from one FTIR scan. A line connecting points represents the interpolated conversion between points.

a very narrow range from 46 to 48%, and did not appear to be substantially influenced by the half-cycle time. Moreover, as the half-cycle time grew shorter, it was found that the conversion profile approached that for continuous exposure at half the intensity (50 μW/cm^2). Apparently, then, for these samples it does not matter much when the free radicals are generated; nearly the same conversion can be achieved.

Figure 3(b), an expansion of the first 15 min of Figure 3(a), shows that at early times there is a separation between the 5-, 10-, 15-, and 30-min half-cycle time curves and that for 1-min half-cycle time. The separation between these curves for the 1- and 5-min half-cycle times suggests that there is a sharp decrease in reactant diffusivity and radical concentration between 1 and 5 min of exposure, followed by a much more gradual decrease at longer times. If the diffusivity and radical concentration had decreased more uniformly with conversion over the entire span between 1 and 30 min, one would expect that all of the curves would have separated from one another. Therefore, it appears likely that the samples have not yet vitrified by the 1-min mark (when the lamp is first turned off for the 1-min half-cycle time sample). However, for times exceeding 5 min, vitrification has likely occurred before the lamp is first turned off. Figure 3(a) shows that at later times, the conversion for the 1-min half-cycle time sample and the continuous exposure for the half-intensity sample gradually increase, to reach about the same conversion as the other cured samples.

Using a 1-min half-cycle time, the first dark periods were introduced at low conversion, when the conversion was still increasing quite rapidly. One can readily detect the departure of this conversion curve from the others at 1 min, when the first dark period was introduced. However, using a 5-min half-cycle time, the first dark period was introduced after about 37% conversion, that is, at such a late time that conversion was not increasing very rapidly. It is not as easy now, however, to detect the departure of this conversion curve from the others at the 5-min time point. In general, the slope of the conversion curves changes less sharply when the first dark reaction time is introduced later in the processing (as the period is increased).

Final Conversion: Diffuse Reflectance IR

Final averaged relative conversions among cured coatings processed in the stress measurement apparatus (obtained using DRIFTS) are shown in Figure 4. The numerical results, along with stan-

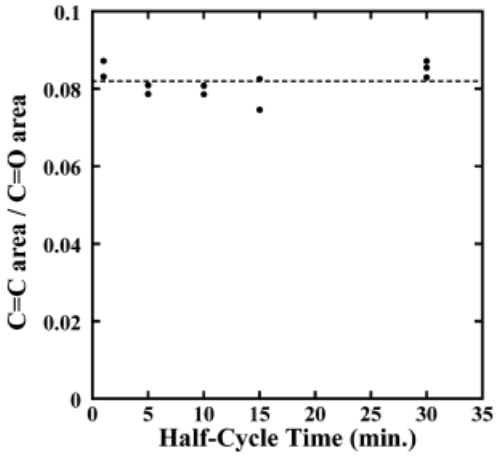

Figure 4 Final relative conversion (DRIFTS) is not affected by the lamp cycling. All samples exposed to cycling had area ratios within 9% of the grand average of 0.082 (represented by dashed line).

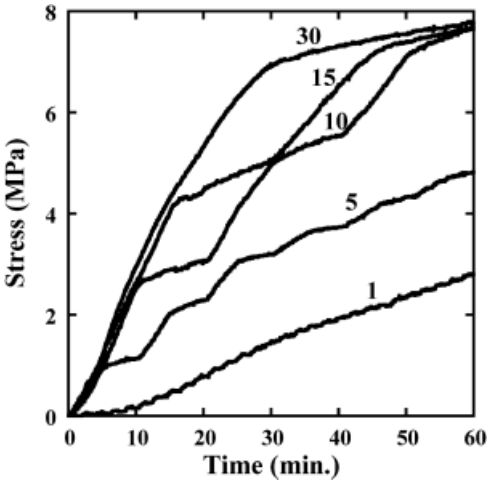

Figure 5 Final stress is affected by the lamp cycling. Plot of residual stress in magnitude, labeling with half-cycle times (in minutes), with total dose = 0.18 J/cm^2 for all cases. Stress for half intensity (limit as half-cycle time $\rightarrow 0$) coating exposed the full hour (not shown) has a final stress of 8 MPa, an indication that the optimal half-cycle time (X) is $0 < X < 5$ min.

dard deviations, are shown in Table I. For all of the coatings prepared with UV cycling, the area ratio was within 9.0% of the grand average (0.082). The Tukey–Kramer analysis ($p < 0.05$) showed that there was not a significant difference in conversion of the coatings prepared in the stress-measurement apparatus. This conclusion is consistent with the transmission FTIR results, which showed only small differences in conversion after cycling was complete. When data for the half-intensity samples (exposed the full time) are included in the statistical analysis, all area ratios were within 8% of the grand average (0.0814) with Tukey–Kramer analysis ($p < 0.05$) still showing no significant differences between samples. Therefore, the DRIFTS tests confirmed the transmission IR results: final conversion of the cured coatings does not depend on the radiation history.

Stress

Figure 5 shows stress as a function of time during the different curing sequences. To point out the most salient features of stress behavior in a crosslinking system, we first focus on the stress profile for a coating exposed to a half-cycle time of 30 min. During the first minute or so, no stress develops because the coating is still a liquid. At this stage, the volume change from shrinkage can be accommodated by flow. The stress-relaxation time during this period is almost instantaneous. However, as the polymerization proceeds further, the elastic modulus of the coating increases and the stress-relaxation rate slows until stress can be supported. After this point, further conversion leads to frustrated shrinkage and, therefore, an increase in coating stress. Although most of the conversion takes place during the first 5 min [see Fig. 3(a)], stress steadily continues to rise after that point because the magnitude of the stress depends not only on shrinkage but also on modulus, which increases significantly as conversion

Table I Final Relative Conversion, Reduced Modulus, and Hardness for the Lamp Cycling X On/X Off Experiments, Where X is the Half-Cycle Time

X (min)	C═C Area/C═O Area	E_r (GPa)	H (GPa)
30	0.0852 ± 0.0021	2.716 ± 0.216	0.1094 ± 0.0061
15	0.0789 ± 0.0033	2.737 ± 0.028	0.1122 ± 0.0002
10	0.0797 ± 0.0016	2.783 ± 0.062	0.1147 ± 0.0003
5	0.0798 ± 0.0016	2.694 ± 0.030	0.1105 ± 0.0016
1	0.0852 ± 0.0029	2.720 ± 0.034	0.1090 ± 0.0017
0 (1/2 intensity)	0.0808 ± 0.0021	2.431 ± 0.308	0.1031 ± 0.0029

proceeds. When the lamp is turned off at the 30-min mark, stress continues to grow, though less quickly. It is difficult to detect stress relaxation during this dark period because, by the time the lamp is turned off, the modulus and stress-relaxation time are large enough that even a small increase in conversion during the dark period will lead to an increase in stress. Instead, it would seem that the change in slope is the result of a slower chemical reaction rate. For the coatings exposed to half-cycle times of 15 and 10 min, the stress behavior is similar to that of the 30-min case. The slopes of these stress curves during the lamp on periods are about the same at any given stage of the process, as are the lamp off periods. Therefore, the final coating stress in all three cases is roughly the same, about 8 MPa.

The stress profile using a half-cycle time of 5 min is quite different. Aside from the first 5 min of radiation, the slopes of the stress curve for this coating during the lamp on and off times are smaller than those for the 30-, 15-, and 10-min half-cycle time coatings. This difference can already be seen at the 20-min time point; at that moment, the 5- and 10-min half-cycle time coatings have been exposed to equal amounts of light and dark. However, the coating exposed to the 5-min half-cycle time has a significantly lower stress than that of the coating exposed to the 10-min half-cycle time. Therefore, using a half-cycle time of 5 min, the final stress reaches only 5 MPa. There are several factors that may contribute to the difference in stress. The modulus of the coating may be lower at a given time, or the conversion itself may also be causing less shrinkage resulting from a different structural development. Both possibilities would result in a lower stress. Furthermore, the lower stress may be attributable to the greater amount of stress relaxation, especially early in the process.

The stress behavior for the coating exposed to a half-cycle time of 1 min is also very different from that for the other coatings. During the first 8 min, very little coating stress is apparent. Dark-period stress relaxation is playing a key role during this time, which can easily be seen in Figure 6. There are clear increases in stress during the lamp on periods (starting at even-numbered minutes) and gradual decreases in stress during the off periods (starting at odd-numbered minutes). Note that at early times and during the lamp off periods, conversion is still increasing, although the modulus of the coating is small. The stress accumulated from the additional conversion is small and stress

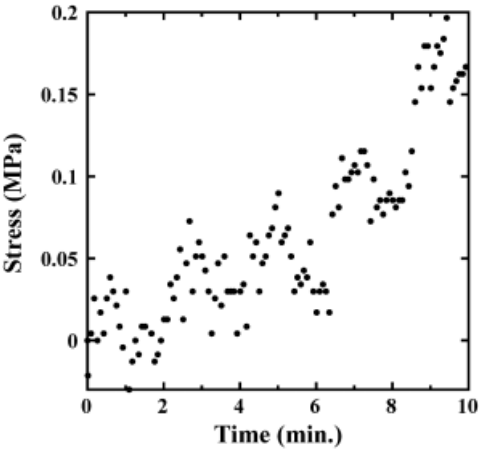

Figure 6 Dark reaction period stress relaxation that is apparent, especially at early times, for the coating exposed to a 1-min half-cycle time. All the data points, acquired every 5 s, are plotted.

relaxation can occur. After about the 8-min point, stress gradually begins increasing with time. Now, the increase in stress during the lamp on times is larger than the relaxation of stress (or slower rate of cure) during the lamp off times. Much later in the processing (after the 40-min time point), decreases in stress are not apparent during the dark reaction periods; instead, there are decreases in slope for the stress curves, just like with the 30-, 15-, 10-, and 5-min half-cycle time coatings. Therefore, later in the processing, changes in slope when the lamp is turned off indicate a slower rate of cure. The final stress for the coating cured with a 1-min half-cycle time is only 3 MPa. Therefore, Figure 5 illustrates that final stress, unlike conversion, depends strongly on the radiation history. One can conclude that there is a characteristic time before which the first dark reaction period must be imposed to be effective in lowering stress.

For the limiting case as the cycling period approaches zero (50 μW/cm^2 and 1 h of continuous exposure), coating stress climbs more slowly but once again reaches 8 MPa (not shown). This value is higher than the final values for 1- and 5-min half-cycle time coatings, suggesting that an optimal curing sequence exists for a given overall dose of radiation. For equal-interval on/off cycling and the above conditions, the optimal cycle time for the present combination of monomer and initiator appears to be between the half-cycle times of 0 and 5 min.

Although conversion profiles shown in Figure 3(a) for half-cycle time $\geq$ 5 min are roughly the

same, their stress profiles shown in Figure 5 are different. Specifically, there are sharp changes in slope for the stress curves when the UV lamp is switched on or off. These changes in slope are not apparent for the conversion curves, which might mean that even a very slight change in strain rate (small change in slope for conversion) may lead to sharp changes in the slopes of the stress curves because the modulus at higher conversions can be large.

In this study, stress relaxation seems to be playing a major role; however, it is not easy at this point to determine *a priori* the stress-relaxation time. For viscoelastic materials, stress-relaxation time may be expressed as[37]

$$\tau = \mu/E \tag{6}$$

where μ and E are the material's viscosity and modulus, respectively. According to Maxwell's model, when a step strain is applied to a viscoelastic sample, stress decays exponentially with time according to

$$\sigma = \sigma_0 e^{-(t/\tau)} \tag{7}$$

Note that it is not possible to directly determine a numerical value for stress-relaxation time by fitting eq. (7) to the dark intervals of the stress curves in Figure 5 because a competing chemical reaction during the dark reaction periods causes strain to change during these intervals. Unfortunately, current theoretical models also cannot be used to estimate the evolution of stress-relaxation time for the conditions in this curing study. Most of these models predict behavior only for linear chains and involve polymeric chain reptation through a three-dimensional network, to determine the diffusion coefficient and stress-relaxation time as functions of polymer molecular weight; the models are inadequate for branched or crosslinked systems.[38] One way to determine the evolution of stress-relaxation time is to perform rheological measurements. If one determined the dependency of modulus and viscosity on frequency, a curve fit would provide the evolution of stress-relaxation time. Such a study is currently under way and will be used to compare the three characteristic times: stress-relaxation time, chemical-reaction time, and cycle time.

This study has shown that, in general, imposing dark reaction periods earlier in the processing is more effective in lowering stress because the stress-relaxation time is shorter than the lamp off time. Presumably, the best way to have both the most stress relaxation and the most chemical reaction would be to have the cycle time proportional to the polymer relaxation time. For a given dose, shorter and more frequent dark periods should be imposed early in the processing when stress-relaxation time is shorter.

Hardness and Modulus

Hardness and modulus values for coatings adhering to cantilever bars are shown in Figures 7 and 8, respectively. These numerical results, along with standard deviations, are shown in Table I. For all of the samples prepared using UV cycling, the hardness was within 6% of the grand average (0.110 GPa), whereas the reduced modulus values were all within 8% of the grand average (2.73 GPa). The Tukey–Kramer analysis ($p < 0.05$) showed that lamp cycling had no significant effect on hardness and modulus. When the half-intensity samples (exposed the full time) were included in the statistical analysis, all hardness values were within 12% of the grand average (0.109 GPa) and all modulus values were within 20% of the grand average (2.65 GPa), with Tukey–Kramer analysis ($p < 0.05$) still showing no significant differences in hardness or modulus between samples. To be even more confident that any differences in hardness or modulus could be revealed, more samples would need to be tested.

The hardness and modulus data obtained for all the samples were within the commonly reported range for acrylate polymers.[39–41] Variations among samples subjected to the same cure pathway could be attributed to differences in the roughness of the surfaces being sampled during the indentation process. Small differences in the local topography can produce discernible deviations in the hardness and the modulus because of the dependency of these parameters on the contact area. Substrate contributions in the results are not important, given that the maximum depth reached during the indentation (1.1 μm) was just about 2% of the film thickness. The so-called substrate effect in nanoindentation becomes significant only when the penetration depth is greater than 20% of the film thickness.[42]

This analysis indicates that there were no significant differences in mechanical properties for coatings prepared by the various cure pathways, which may have been predicted given the conversion results. Therefore, although the processing

stresses are found to decrease with the radiation cycle time, the final properties of the coatings are virtually unaffected. Therefore, by cycling the radiation, stress in the coating can be reduced without incurring a commensurate reduction in final properties.

CONCLUSIONS

This study showed that by cycling a UV lamp on and off, keeping the total dose constant, it is possible to achieve the same conversion, hardness, and modulus, but with lower stress. Stress and conversion results are summarized in Figure 9. Stress was lowered from 8 MPa to less than 3 MPa as the half-cycle time was decreased from 30 to 1 min. When the sample was exposed to half intensity for the full amount of time (the limit as the period $\rightarrow 0$), final stress reached 8 MPa, an indication that for the conditions chosen in this study, the optimal half-cycle period is between 0 and 5 min. It is not clear whether the 1- and 5-min half-cycle time coatings might reach similar stress values as those of the other coatings upon aging, but it is nevertheless clear that a lower stress is attained even at the same conversion.

When UV exposure is cycled, the chemical reaction response time, polymer-relaxation time, and cycle time period are all key parameters determining the final stress. From this study, one may conclude that to optimize UV-cure, the cycle time should be proportional to the stress-relaxation time. This would mean that the cycling period should increase with increasing conversion (and hence, increasing relaxation time). A study is currently under way to examine these prospects.

A half-cycle time of 1 min was the best curing sequence investigated thus far because conversion remained close to 47% and final stress was less than 3 MPa. However, this curing sequence is most likely not the optimal one. There are infinite

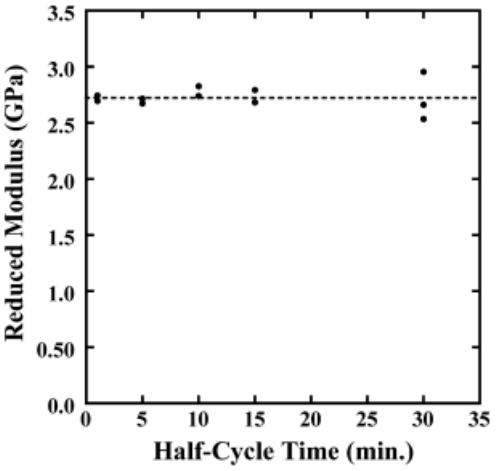

Figure 8 Reduced modulus is not affected by the lamp cycling. All samples exposed to cycling had reduced modulus values within 8% of the grand average of 2.73 GPa (represented by dashed line).

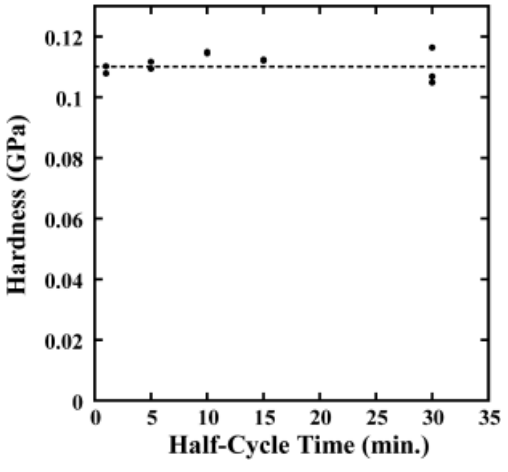

Figure 7 Hardness is not affected by the lamp cycling. All samples exposed to cycling had hardness values within 6% of the grand average of 0.110 GPa (represented by dashed line).

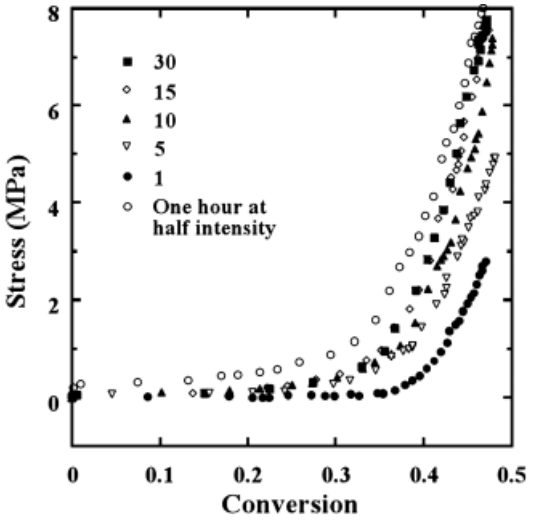

Figure 9 Summary of residual stress and conversion results, labeling with half-cycle times, for the lamp cycling study.

ways of carrying out an exposure sequence. A model is currently being formulated to point out key experiments that can be used in the optimization of UV cure.

The authors acknowledge financial support from the Industrial Partnership for Research in Interfacial and Materials Engineering at the University of Minnesota, through its Coating Process Fundamentals Program, and the Intel Corp; the technical assistance of K. Zhang and J. Nelson; and the helpful discussions with C. Miller, W. W. Gerberich, and S. Weisberg.

REFERENCES

1. Wilson, T. W.; Turner, D. T. J Dent Res 1986, 66, 1032.
2. Kloosterboer, J. G. Adv Polym Sci 1988, 84, 1.
3. Pappas, S. P., Ed. Radiation Curing: Science and Technology; Plenum: New York, 1992.
4. Wicks, Z. W.; Jones, F. N.; Pappas, S. P., Eds. Organic Coatings: Science and Technology; Wiley: New York, 1994; Vol. II, p 253.
5. Croll, S. G. J Coat Technol 1978, 50, 33.
6. Sato, K. Prog Org Coat 1980, 8, 143.
7. Perera, D. Y.; Vanden Eynde, D. J Coat Technol 1984, 56, 47.
8. Payne, J. A.; Francis, L. F.; McCormick, A. V. J Appl Polym Sci 1997, 66, 1267.
9. Stolov, A. A.; Xie, T.; Penelle, J.; Hsu, S. L. Polym Mater Sci Eng 2000, 82, 371.
10. Eliades, G. C.; Vougiouklakis, G. J.; Caputo, A. A. Dent Mater 1987, 3, 19.
11. Tong, K.; Taylor, J. F.; Farris, R. J. Mater Res Soc Symp Proc 1991, 226, 109.
12. Best, M. E.; Prime, R. B. Proc SPIE Int Soc Opt Eng 1992, 1774, 169.
13. Walls, A. W. G.; McCabe, J. F.; Murray, J. J. J Dent Res 1988, 16, 177.
14. Lai, J. H.; Johnson, A. E. Dent Mater 1993, 9, 139.
15. Watts, D. C.; Cash, A. J. Dent Mater 1991, 7, 281.
16. Wen, M.; Ng, L. V.; Payne, J. A.; Francis, L. F.; Scriven, L. E.; McCormick, A. V. in Proceedings of the 50th Annual Conference of the Society for Imaging Science and Technology, Cambridge, MA, May 1997; p 564.
17. Kloosterboer, J. G.; Van de Hei, R. G. Polym Commun 1984, 25, 322.
18. Kloosterboer, J. G.; Lijten, G. F. C. M.; Zegers, C. P. G. Polym Mater Sci Eng 1989, 60, 122.
19. Anseth, K. S.; Wang, C. M.; Bowman, C. N. Polymer 1993, 35, 3243.
20. Anseth, K. S.; Bowman, C. N.; Peppas, N. A. J Polym Sci Part A: Polym Chem 1994, 32, 139.
21. Anseth, K. S.; Wang, C. M.; Bowman, C. N. Macromolecules 1994, 27, 650.
22. Flory, P. J. Principles of Polymer Chemistry; Cornell University Press: Ithaca, NY, 1953; p 148.
23. Odian, G. Principles of Polymerization, 3rd ed.; Wiley: New York, 1992; p 270.
24. Payne, J. A.; Francis, L. F.; McCormick, A. V. Rev Sci Instrum 1997, 68, 4564.
25. Stoney, G. G. Proc R Soc London 1909, A82, 172.
26. Timoshenko, S. P.; Gere, J. M. Theory of Elastic Stability; McGraw-Hill: New York, 1961; p 257.
27. Corcoran, E. M. J Paint Technol 1969, 41, 635.
28. Dumont, N.; Depecker, C. Vib Spectros 1999, 20, 5.
29. Moradi, K.; Depecker, C.; Corset, J. Appl Spectrosc 1994, 48, 1491.
30. Bushan, B.; Kulkarni, A. V.; Bonin, W. A.; Wyrobek, T. Philos Mag A 1996, 74, 1117.
31. Doerner, M. F.; Nix, W. D. J Mater Res 1986, 1, 601.
32. Anseth, K. S.; Decker, C.; Bowman, C. N. Macromolecules 1995, 28, 4040.
33. Larson, E. G.; Spencer, D. S.; Boettcher, T. E.; Melbauer, M. A.; Skarjune, R. P. Radiat Phys Chem 1987, 30, 11.
34. Cook, W. D. Polymer 1992, 33, 2152.
35. Dietz, J. E.; Peppas, N. A. Polymer 1997, 38, 3767.
36. Goodner, M. D.; Lee, H. R.; Bowman, C. N. Ind Eng Chem Res 1997, 35, 1247.
37. Young, R. J.; Lovell, P. A. Introduction to Polymers; Chapman & Hall: London, 1991; p 326.
38. Sperling, L. H. Introduction to Physical Polymer Science; Wiley: New York, 1992; p 181.
39. Steffen, U.; Alberts, H.; Prinz, R. Ger. Pat. 2811549, 1979.
40. Schellenberg, J.; Hamann, B. Ger. Pat. 267504, 1989.
41. Hongo, H.; Hitoyasu, H.; Hatsutori, T.; Hayamizu, S.; Nozawa, M.; Iwata, H. Jpn. Pat. 08292328, 1996.
42. Strojny, A.; Xia, X.; Tsou, A.; Gerberich, W. W. J Adhes Sci Technol 1998, 12, 1299.